Proceedings of ASME PVP:
COMPUTATIONAL TECHNOLOGY (CFD)
FOR FLUID/THERMAL/CHEMICAL/STRESS SYSTEMS
AND INDUSTRIAL APPLICATIONS
July 22-26, 2001 Hyatt Regency, Atlanta, Georgia, USA

NUMERICAL SIMULATION OF WATER FLOW AROUND SHIP WITH SCREW PROPELLER

Andrey Aksenov, **Victor Pokhilko** **Alexander Dyadkin**

TESIS Co., off 701-703, Unnatov 18, Moscow, Russia, 125083,
E-mail: flowvision@tesis.com.ru

ABSTRACT

This paper outlines development of method for simulation of complex fluid flows having arbitrary motion of free surfaces. The method is based on rectangular grid with dynamic local grid adaptation. For approximation of a curvilinear computational domain boundaries and a free surface the subgrid geometry resolution method is used. The free surface tracking is provided by VOF method.

Using this approach a fluid flow around ship hull is simulated. Calculation is made with and without taking into account screw propeller. Results are compared with experiment.

INTRODUCTION

Friction force is the main characteristic of a ship. In practice this characteristic is defined experimentally using small scalable model of the ship. Unfortunately it is impossible to scale all main effects of ship motion in small model – turbulent boundary layer, wave generation and action of screw propeller. Now an application of numerical simulation for ship design promises to take into account all effects of ship motion simultaneously. To accurately simulate the water flow around ship a lot of problems must be resolved. Approximation of ship curvilinear body and tracking of water free surface are among these problems. Ordinary solution approach consists in using curvilinear grid fitted to ship body and to water surface. This approach has two main difficulties– it is hard to simulate wave breakdown near nose of a ship and a lot of computation time is needed for grid regeneration at each time step. Alternative approach is VOF method. Disadvantage of this method is the need of solution extrapolation onto the "surface" cells. This is the main source of errors and instabilities.

In this paper we offer an extension of VOF approach (Hirt, Nichols, 1981). It is realized in ***FlowVision*** CFD code (Aksenov A. et al., 1996). Our approach is based on modified finite volume method and Cartesian calculation grid with local adaptation. Curvilinear shape is approximated by subgrid geometry resolution method (Aksenov A. et al., 1998). Shape is represented by a set of plane facets in this method. Grid cell crossed by boundary is cut off and transformed from parallelepiped to polyhedron.

Extension of VOF method consists in reconstruction of free surface from VOF function inside calculation cell. Surface is represented by set of plane facets to be suitable for approximation by subgrid geometry resolution method.

Two models of dry cargo ship, with and without screw propeller, are simulated using this approach. Screw propeller is modeled by disk that has water inflow from one side and water outflow from another side. Good coincidence of experimental

and simulated results is obtained proving for correctness of the used approach.

NOMENCLATURE

t	-	time,
τ	-	time step,
f	-	any calculated variable,
P	-	pressure,
$\mathbf{V}$	-	fluid velocity,
k	-	turbulence energy,
ε	-	turbulence energy dissipation,
μ	-	molecular viscosity;
μ_t	-	turbulent viscosity;
l	-	length scale of turbulence,
ρ	-	fluid density,
ρ_{ref}	-	reference fluid density,
S	-	square of free surface in cell,
$\mathbf{n}$	-	normal to free surface in cell,
$\mathbf{n}_d$	-	d-th ort of coordinate system,
$\mathbf{N}$	-	normal to computational domain boundary,
$\mathbf{g}$	-	gravity force,
z	-	coordinate in direction of $\mathbf{g}$;
z_0	-	z-coordinate of undisturbed water surface,
y	-	distance from point in fluid and boundary,

MATHEMATICAL MODEL

Governing Equations. Mathematical model of incompressible water flow around the ship consists of mass conservation law, Navier-Stokes equations and k-ε model of turbulence:

$$\frac{\partial \mathbf{V}}{\partial t} + \nabla(\mathbf{V} \otimes \mathbf{V}) = -\frac{\nabla P}{\rho} + \frac{1}{\rho}\nabla((\mu + \mu_t)(\nabla \mathbf{V} + (\nabla \mathbf{V})^T) + \mathbf{g} \quad (1)$$

$$\nabla \mathbf{V} = 0$$

$$\frac{\partial k}{\partial t} + \nabla(\mathbf{V}k) = \frac{1}{\rho}\nabla((\mu + \frac{\mu_t}{\sigma_k})\nabla k) + \frac{G}{\rho} - \varepsilon$$

$$\frac{\partial \varepsilon}{\partial t} + \nabla(\mathbf{V}\varepsilon) = \frac{1}{\rho}\nabla((\mu + \frac{\mu_t}{\sigma_\varepsilon})\nabla \varepsilon) + \frac{\varepsilon}{k}(C_1 \frac{G}{\rho} - C_2 \varepsilon)$$

where

$$\mu_t = C_\mu \rho \frac{k^2}{\varepsilon},\ G = \mu_t \frac{\partial V_i}{\partial x_j}(\frac{\partial V_i}{\partial x_j} + \frac{\partial V_j}{\partial x_i})$$

σ_k =1,0; σ_ε =1,3; C_μ =0,09; C_1 =1,44; C_2 =1,92

To simplify boundary conditions and to avoid round-off errors, the pressure is split into two parts – hydrostatic P_H and dynamic P_D pressure

$$P = P_H + P_D. \quad (2)$$

Let direction of gravity vector be along z coordinate, so that

$$P_H = \rho_{ref}\, g\, (z - z_0) \quad (3)$$

If $\rho = const = \rho_{ref}$, then equations (1) can be written in next form

$$\frac{\partial \mathbf{V}}{\partial t} + \nabla(\mathbf{V} \otimes \mathbf{V}) = -\frac{\nabla P_H}{\rho} + \frac{1}{\rho}\nabla((\mu + \mu_t)(\nabla \mathbf{V} + (\nabla \mathbf{V})^T)$$

Boundary Conditions. A computational domain is shown in Figure 1. A half of ship is considered. Boundary conditions specified at domain borders are following:

"**In**" – inflow of water in computational domain:

$$\boldsymbol{V}|_{In} = \boldsymbol{V}_{ship}$$
$$k|_{In} = 0.0025*(V_{ship})^2$$
$$\varepsilon|_{In} = C_\mu (k|_{in})^{3/2} / l$$

where $\boldsymbol{V}_{ship}$ is the ship velocity, $l \approx 0.01 \div 0.1L$, where L is transverse size of the ship.

At boundaries "**Out**" and "**Brd**" a pressure boundary condition is specified

$$P_H|_{Out,\,Brd} = 0$$
$$df/dy|_{Out,\,Brd} = 0,$$

note, that boundary condition "**Brd**" is specified also at bottom of computational domain.

Boundary "**Sym**" is the symmetry boundary condition

$$df/dy|_{Sym} = 0.$$

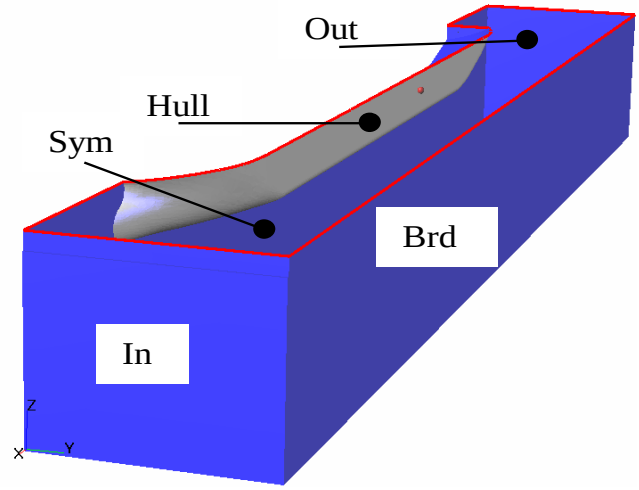

Figure 1. Computational domain

At ship hull the logarithmic law boundary condition (Sondak, Pletcher, 1995) with shear stress is specified

$$\tau_w = \mu_t \left.\frac{\partial U}{\partial y}\right|_{y=0}$$

here, velocity inside the turbulent boundary layer is assumed to obey the equation

$$\frac{U}{U_*} = \frac{1}{\kappa}\ln\left(\frac{\rho U_* h}{\mu} E\right),$$

where $U_* = \sqrt{\frac{\tau_w}{\rho}}$, κ = 0.41, E=9.

Values of k and ε are defined in grid cells near the ship hull via expressions

$$k_i = \frac{U_*^2}{\sqrt{C_\mu}},\ \varepsilon_i = \frac{1}{\kappa}\frac{U_*^3}{y_i},$$

where y_i is distance between the center of *i*-th grid cell and the ship hull.

At free surface for all variables except pressure the zero gradient boundary conditions are specified

$$df/dy|_{free} = 0.$$

The pressure is equal to zero

$$P|_{free} = 0, \quad (4)$$

From (2-4) we find the dynamic pressure boundary condition

$$P_D|_{free} = -\rho_{ref}\, g\, (h - z_0),$$

Where *h* is the free surface vertical position.

NUMERICAL APPROACH

Method of Modified Finite Volumes.

Numerical method used in this paper is method of modified finite volumes (MMFV). This method is described in (Aksenov et al., 1998) and we won't describe it here in details. MMFV is based on rectangular calculation grid. Rectangular grid can be adapted by dividing each cell into 8 different cells.

The boundaries of computational domain are presented by a set of plane facets (surface mesh). If boundary crosses grid cell, initial cell is split into other cells that are polyhedrons. So the new cells are bounded by part of initial cell faces and boundary surface mesh. Governing equations are approximated on this grid without any simplifications of cell geometry (Subgrid Geometry Resolution method, see also (Aksenov et al., 1998)).

Navier-Stokes equations are solved by split method (Belotserkovsky, 1994) that was advanced for implicit scheme in (Aksenov et al. 1996a, Aksenov et al. 1996b). Convective transfer terms in governing equations is approximated by numerical scheme described in (Aksenov et al., 1993, Aksenov et al., 1996b)

Free Surface Tracking.

"Volume of fluid" method (VOF) is used for tracking the free surface. Designate F as relative part of grid cell volume occupied by fluid phase. The cell is filled by fluid entirely if F equals 1 (we shall call it "fluid cell") and is filled by gas if F equals zero ("gas cell"). If F is between 0 and 1, then the cell is crossed by a free surface ("free surface" cell).

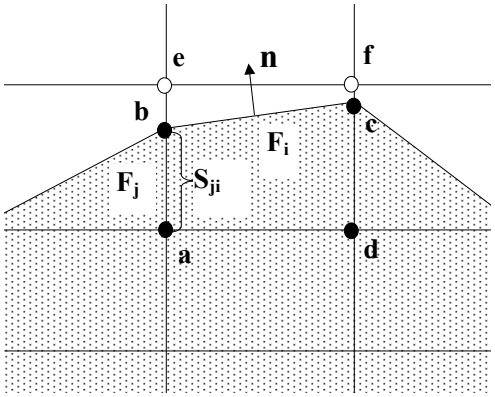

Figure 2. Reconstruction of free surface cell via VOF function F.

The simulation of free surface flows by use of VOF method can be split into two problems. The first one is transferring F over calculation grid with known fluid velocity. The second problem is approximation of governing equations in free surface cells. Here we concentrate on the last problem.

Original VOF method or its modifications (Hirt, Nichols, 1981) solve governing equations over fluid cells only. Free surface cells are used as boundary conditions. An extrapolation is used to find the solution inside the free surface cells. Our practice of application of VOF method in this form for simulating the ship motion problems shows that this method gives rather big errors when defining the ship wave resistance. The source of errors lays in the method of data extrapolation from fluid cells to free surface cells.

The idea of proposed method consists in solving the mathematical model equations in the free surface cells as well. Geometry of free surface cells

is defined using function F. Initial *aefd* cell is cut by free surface and transformed to *abcd* cell (Figure 2). If neighbor of the free surface cell is fluid cell, the face between them does not vary. If neighbor is gas cell, the face area is specified to zero. Face area between two free surface cells i and j is equal $S_{ij} = 0.5*(F_i+F_j)$. Volume of the free surface cell is specified via Gauss theorem through cell faces instead of evident multiplying volume of *aefd* cell by F_i. We need this to ensure realization of Gauss theorem during approximation of governing equations. Square S and normal **n** of free surface in the cell are defined through square faces of the cell:

$$S = \sqrt{\sum_{d=1}^{3} (S_{id_o} - S_{id_1})^2}$$

$$\mathbf{n} = \sum_{d=1}^{3} \mathbf{n}_d (S_{id_o} - S_{id_1}) / S$$

here d_0 and d_1 are indexes of the neighboring cell in direction d to the cell i.

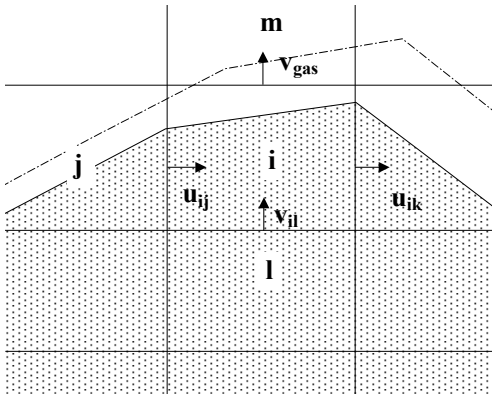

Figure 3. Calculating velocity at faces between free surface and gas cells.

Let function F and all variables be known at time t^n. Variables at t^{n+1} are calculated by applying the following procedure:

1) All grid cells are marked as "fluid", "gas" or "free surface" cells.

2) Velocities v_{gas} (Figure 3) at faces between free surface cells and gas cells are defined using the mass conservation law. If faces are more then one, mass fluxes between them are distributed proportionally to the scalar product of velocity in the free surface cell and normal to the gas cell face $\mathbf{V}\,\mathbf{n}_d$.

3) Explicit convective transfer of function F between the free surface cells and their neighbors is calculated, and F^{n+1} is defined. Also, explicit convective transfer of calculated variables is defined in gas cells.

4) New geometry of free surface cells is reconstructed.

5) Governing equations are solved for new shape of computational domain.

RESULTS

Figure 4 Hull of dry cargo ship.

Simulation of water flow is performed for dry cargo ship designed in "Vympel" company (Niznii Novgorod, Russia). Its hull is shown in Figure 4. A model of this ship was tested in the pool of "Vympel" company. The comparison against the experimental results will be done below.

Simulation is performed for ship with and without screw propeller. Screw propeller is modeled by double side disc. Water inflows through one side and outflows through another side of disc with some velocity.

Computational grid is shown in Figure 5. The grid is refined to water surfaces in vertical direction, to nose and stern along ship. Also grid is refined at the sides of the ship (in perpendicular direction to the figure). Grid is adopted for one level over all hull and two levels near the screw propeller (for calculations with propeller).

A water surface (bow and quartering seas) is shown in Figure 6. In (a) one can see waves near ship without screw propeller, in (b) – with propeller. It is evident, that bow sea is not affected by propeller. But shape of quartering sea depends on whether propeller is taken into account. Screw propeller creates the zones of low pressure before and high pressure after it. This effect results in slight increase of wave height behind ship and increase of wave depth before propeller near the stern.

The wetted surface of the ship hull as function of ship speed and screw propeller is shown in Figure 7. One can see the maximum height of upper wetted surface is on the ship nose. Water surface is almost plane at speed less then 5 mph, for these cases the simulation of water flow can be done without taking into consideration the free surface disturbance (Chicherin, Lobachev, 2000).

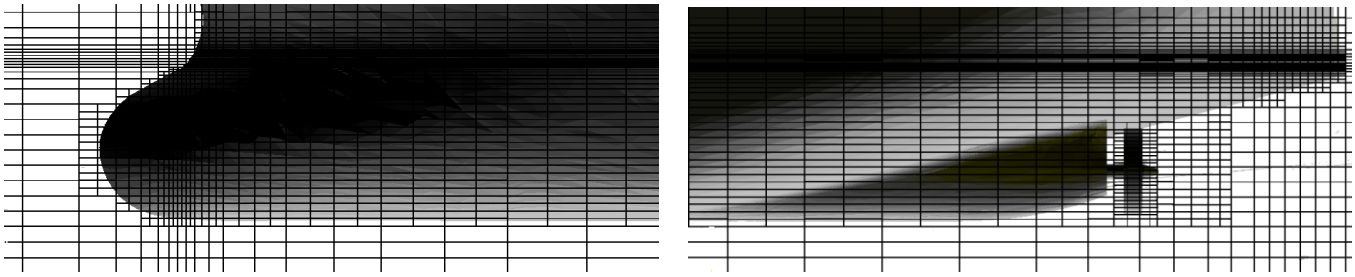

Figure 5 Calculation grid near nose and stern of the ship.

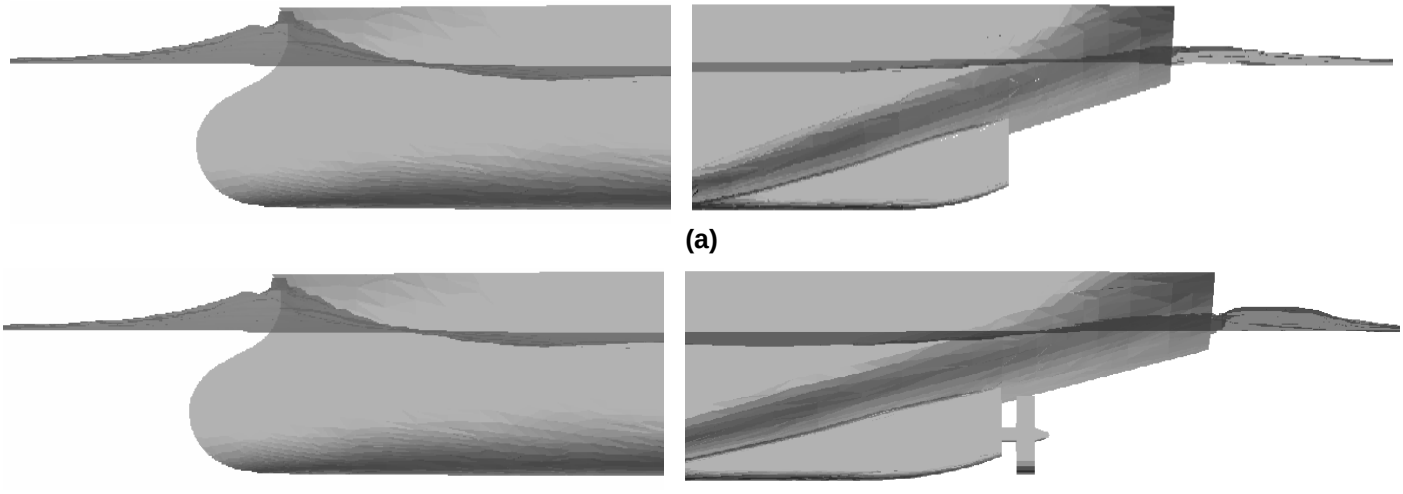

(a)

(b)

Figure 6 Water surface near nose and stern of the ship.

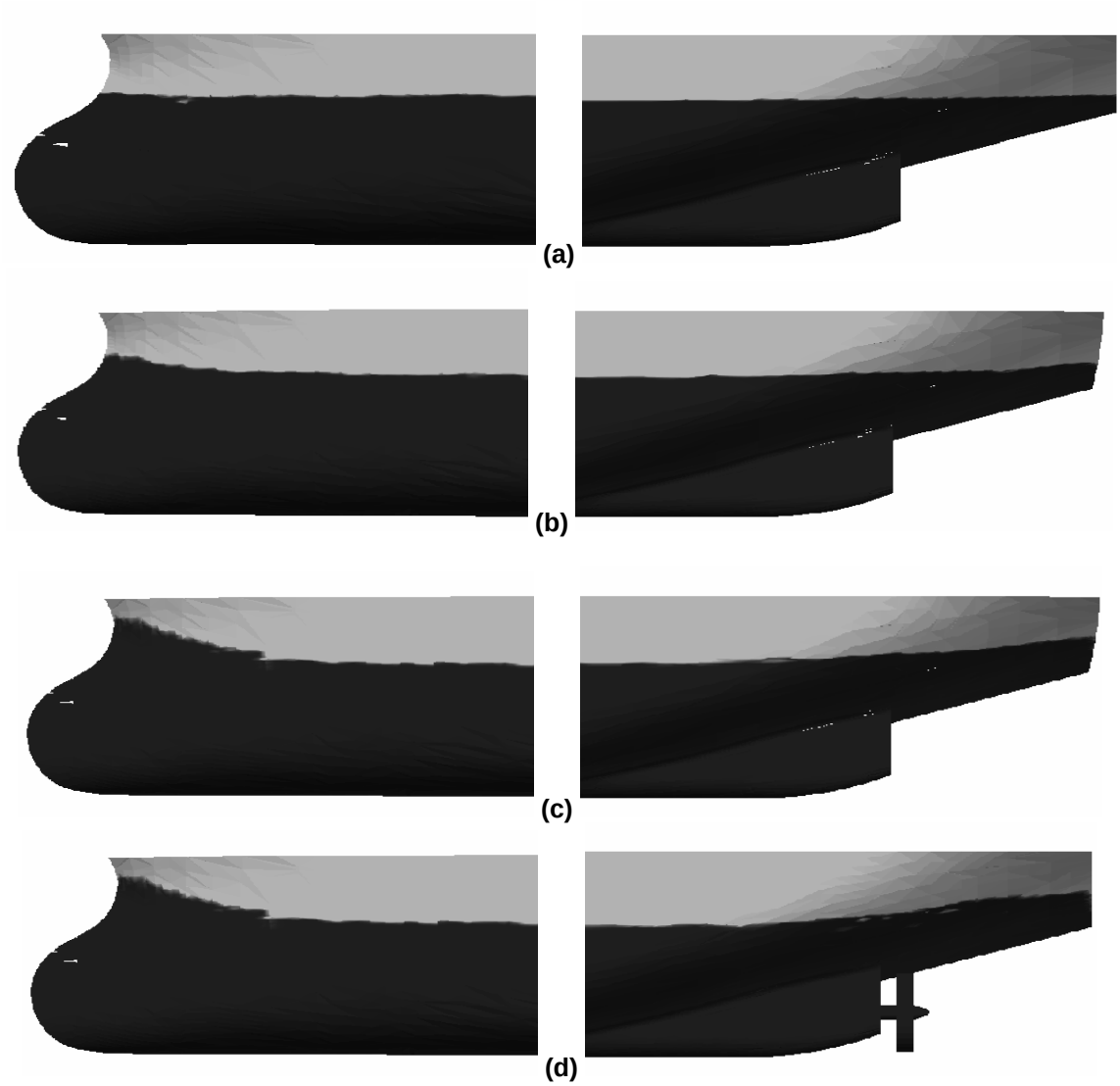

Figure 7 Wetted surface of ship hull near nose and stern. Speed of the ship: (a) – 5 mph, (b) – 8 mph, (c) – 11 mph and (d) - 11 mph with screw propeller taken into account.

Let's introduce density function of drag Π_x and lift Π_z pressure forces

$$\Pi_x = \oint_{L(x)} N_x P_D dl\,, \quad \Pi_z = \oint_{L(x)} N_z P_D dl$$

where *L(x)* is the cross-section contour at *x=const*, *x* is the direction along ship, *z* is the vertical direction. This density function of pressure force shows distribution of drag and lift along ship hull. Note, that integration of Π_x and Π_z along *x* gives drag and lift force on ship (without viscous friction).

Drag density Π_x is shown in Figure 8. The maximum drag density is along nose (Figure 8, a). Big negative values correspond to flow braking at nose. The positive values of drag density (accelerating forces) correspond to drop of water level just behind the nose (see Figures 6, 7). Contribution of stern in drag force is small – there are positive and negative force density values annulling each other. Screw propeller (dashed line in Figure 8, b) changes balance of drag-accelerating forces in stern region. Appearance of pressure discharging before propeller results in increasing negative component of pressure density that leads to overall drag increase.

Lift force density is shown in Figure 9. Note, that here is dynamic component of lift excluding

Archimedean force. You can see, that propeller action results in increasing negative lift over stern. It leads to increasing ship pitch for rotating propeller compared to the idle one.

Simulation of fluid flow around ship was compared with experiments for the ship without propeller. Experiments were performed for ship model and data were recalculated for real ship. Simulated and experimental results of ship friction force as function of the ship speed are shown in Figure 10. Both results have good coincidence, with error less then 5%.

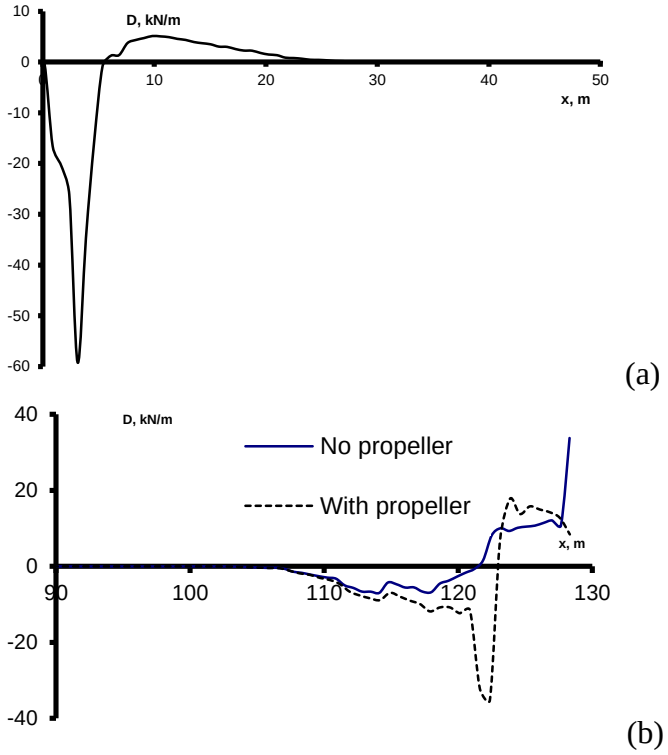

Figure 8 Drag density. Speed of the ship 11 mph, (a) – ship nose, (b) – stern.

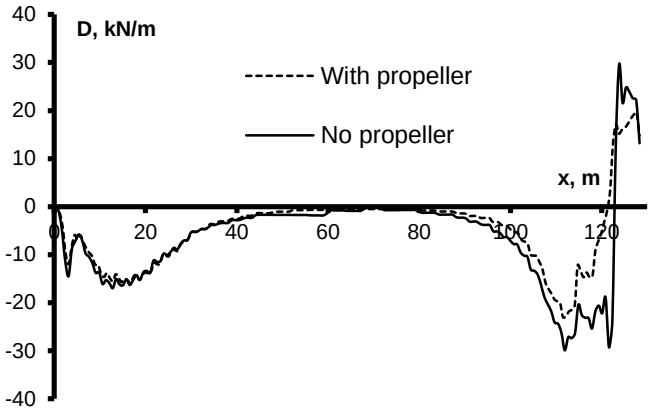

Figure 9 Lift density. Speed of the ship 11 mph.

Unfortunately, the experimental facility couldn't supply the experimental study of the ship with rotated screw propeller. Calculated data is shown in Figure 11. Speed of ship is 11 mph. Simulation is performed for different velocity of water flow through screw propeller. In this figure the water velocity is defined relative to the ship speed. There are two forces: "Drag" is force acting only on the ship hull except the screw propeller, and "Resultant" is the overall force affected on both ship hull and propeller. If the ship is moving with constant speed, resultant force must be zero.

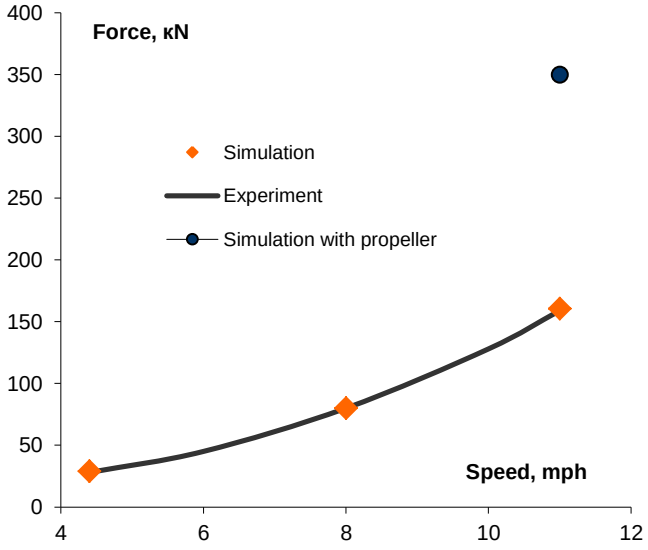

Figure 10 Dependence of friction force on ship speed.

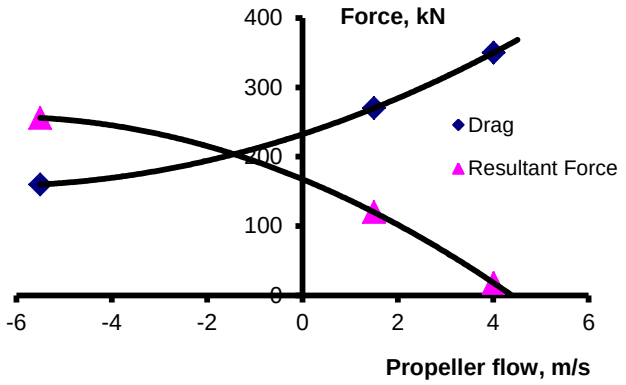

Figure 11 Dependence of ship friction force on water velocity through propeller.

Zero resultant force occurs at water velocity through propeller 4.1 m/c. Drag force is significantly increased (more than by 2 times) in comparison with the case of the ship without propeller. Explanation of this effect lays in decreasing pressure in stern region caused by screw propeller (see Figure 8, b).

CONCLUSION

The method of modified finite volumes is applied to free surface flows around ship. Comparison with experiment shows good coincidence of proposed method and experimental results. Note that accuracy of simulation is sufficient for use the results in industry for ship design. The simulation gives more information for engineer then experiment. Local values of pressure, velocity, and turbulence characteristics on ship hull or around it can be extracted from simulation; these values can be easily handled to get different distributive characteristics like drag or lift densities, vector of resultant force or momentum.

Influence of screw propeller on ship drag force is studied. Propeller is modeled by disc with two sides through which water inflows and outflows. Water velocity through propeller is determined at zero resultant force affecting ship. The large increase of drag for working propeller is found. Discharging of pressure before screw propeller causes the drag increase.

ACKNOWLEDGMENTS

The authors express their thanks to Dr. U. Rabazov, Dr. V. Shatalov and Dr. V. Tseperstein for attention to this work and experimental results provided for dry cargo ship. Also authors are grateful to Mr. V. Snegovsky for reading the paper and giving a lot of useful remarks.

REFERENCES

Hirt C., Nichols B. 1981, "Volume of Fluid (VOF) method for the dynamics of free boundaries", J.Comput. Phys. v. 39, pp 201-225.

Sondak D., Pletcher R., 1995, "Application of Wall Functions to Generalized Nonorthogonal Curvilinear Coordinate Systems" AIAA Journal, Vo.33, No 1, pp.33-41.

Aksenov A.A., Gudzovsky A.V., Serebrov A.A., 1993, "Electrohydrodynamic Instability of Fluid Jet in Microgravity", 19-24, in Proc. of 5th Int. Symposium on Computational Fluid Dynamics (ISCFD), Aug. 31 - Sept. 3, 1993, Sendai, Japan, Japan Society of Computational Fluid Dynamics, Vol.1, 1993.

Belotserkovsky, 1994 Numerical Methods in Continuum Mechanics, Moscow, Fizmatlit, 2nd edition, p.441.

Aksenov A.A., Gudzovsky A.V., Dyadkin A.A., Tishin A.P., 1996a, "Gaz mixing of Low Head Jet in Crossflow", 67-74, Izvestia of Russian Academy of Sciences, Mechanics of Fluids and Gas, 3 (in Russian).

Aksenov A.A., Dyadkin A.A., Gudzovsky A.V., 1996b, "Numerical Simulation of Car Tire Aquaplaning". Computational Fluid Dynamics '96, J.-A. Desideri, C.Hirsch, P.Le Tallec, M.Pandolfi, J.Periaux edts, John Wiley&Sons, pp. 815-820.

Aksenov A, Dyadkin A, Pokhilko V. Overcoming of Barrier between CAD and CFD by Modified Finite Volume Method, Proc. 1998 ASME Pressure Vessels and Piping Division Conference, San Diego, ASME PVP-Vol. 377-1., 1998

Chicherin I., Lobachev M, 2000, "Application of RANS-CODE to Ship Designing Practical Problem", International Maritime Association of Mediterranean IX Congress IMAM'2000 Proc. 2-6 Apr. 2000, vol. III: Ses I – Napoli, 2000, p. 1-8.